Inorganic Chemistry

Article

Cite This: Inorg. Chem. 2017, 56, 12712-12718

pubs.acs.org/IC

Pr_2FeCrO_6: A Type I Multiferroic

Nibedita Das,[†] Satyendra Singh,[‡] Amish G. Joshi,[∥] Meganathan Thirumal,[#] V. Raghavendra Reddy,[§] Laxmi Chand Gupta,[†,+] and Ashok Kumar Ganguli*[,†,∇]

[†]Department of Chemistry, Indian Institute of Technology Delhi, Hauz Khas, New Delhi 110016, India

[∇]Institute of Nano Science and Technology, Sector 24, Mohali, Punjab 160062, India

[‡]Centre for Nano Science, Jawaharlal Nehru University, New Delhi 110067, India

[∥]CSIR National Physical Laboratory, Dr. K. S. Krishnan Road, New Delhi 110012, India

[§]UGC−DAE Consortium for Scientific Research, Indore 452001, India

[#]Department of Chemistry, University of Delhi, Delhi 110007, India

ABSTRACT: We synthesized double perovskite Pr_2FeCrO_6 by solid-state method. Analysis of its X-ray powder diffraction shows that the compound crystallizes in a centrosymmetric structure with space group *Pbnm*. Our X-ray photoelectron spectroscopy (XPS) studies show that all the cations are present in +3 oxidation state. Magnetization studies of Pr_2FeCrO_6 show that the material is paramagnetic at room temperature and undergoes a magnetic transition below T_{CM} = 250 K. We observe clear magnetic hysteresis loop, for example, below 150 K. A low remnant magnetization M_r, ~0.05 μ_B/f. u., is inferred from the observed magnetic hysteresis loop. ^{57}Fe Mössbauer study at 25 K shows a high hyperfine magnetic field of ~53 T at the Fe nucleus, which corresponds to a magnetic moment of ~6−7 μ_B/Fe. These two results together suggest a ferrimagnetic (nearly compensated or canted) ordering of the Fe moments. Mössbauer studies close to the ferrimagnetic ordering temperature suggest interesting magnetic relaxation effects. A dielectric anomaly observed at T_{CE} = 453 K signals a ferroelectric ↔ paraelectric phase transition. We observe at room temperature a clear and well-defined ferroelectric hysteresis loop, P_S = 1.04 μC/cm^2, establishing ferroelectricity in the material. From these results, we conclude that Pr_2FeCrO_6 is a type I multiferroic ($T_{CE} > T_{CM}$).

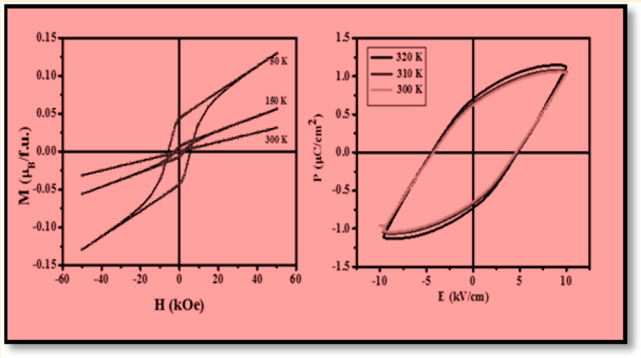

INTRODUCTION

Multiferroics are materials that exhibit simultaneously any two, or more than two, ferroic properties, such as ferroelectricity, ferroelasticity, ferromagnetism (antiferromagnetism), etc.[1,2] Among them, the most extensively studied multiferroics are those that exhibit, below certain temperature, coexisting ferromagnetism and ferroelectricity. This is because such materials (i) are potential candidates for future technologies and (ii) often exhibit features that are quite challenging to understand. Multiferroics are of two varieties: type I multiferroics exhibit ferroelectric transition at a temperature T_{CE} higher than the ferromagnetic transition temperature T_{CM}; that is, $T_{CE} > T_{CM}$. They have high polarization P and also high T_{CE}. Type II multiferroics are characterized by $T_{CM} > T_{CE}$. In such materials ferroelectricity is regarded as induced magnetically,[3] which makes them particularly interesting and challenging. Such materials usually have low polarization P_S and low T_{CE}. In this work, we are concerned with disordered double perovskite multiferroics $R_2BB'O_6$ [where R = Y or a rare-earth element, and B and B′ are transition elements]. Table 1 shows several reported double perovskite multiferroics of type I and type II.[4−13]

Rajeswaran et al.[8] reported multiferroic properties of Y_2FeCrO_6, T_{CM} = 260 K and occurrence of ferroelectricity at and below magnetic transition temperature. Occurrence of ferroelectricity in the material was determined from the measurements of dielectric constant and spontaneous electric polarization measured using dielectric and pyroelectric measurements. Ferroelectric hysteresis loop was not reported in this work. We undertook the synthesis of a related material, namely, Pr_2FeCrO_6, which we describe here. A noteworthy aspect of Pr_2FeCrO_6 is that we observe a clear ferroelectric hysteresis loop at room temperature establishing its ferroelectric nature. It is important to note that though several double perovskites of the type $RE_2BB'O_6$ with multiferroic properties are known, observation of a ferroelectric hysteresis loop of this clarity has been rarely reported in these double perovskites.

EXPERIMENTAL SECTION

Polycrystalline Pr_2FeCrO_6 was prepared by solid-state sintering method. Stoichiometric mixture of the oxides Pr_6O_{11}, Fe_2O_3, and

Received: April 29, 2017
Published: October 6, 2017

DOI: 10.1021/acs.inorgchem.7b01086
Inorg. Chem. 2017, 56, 12712−12718

Table 1. Some Double Perovskite Oxides with Multiferroic Properties

double perovskite	T_{CE} (K)	T_{CM} (K)	space group (temp)	structure	reference
		type I multiferroics			
Bi_2NiMnO_6	485	140	$C2 \rightarrow P2_1/n$ (300→500 K)	ordered	4
Bi_2NiTiO_6	513	58	$Pn2_1a$ (RT)	ordered	5
Y_2FeMnO_6 (single crystal)	328	245, 328, 358	$Pnma$ (RT)	disordered	6
Y_2CrMnO_6 (single crystal)	390	74	$Pnma$ (RT)	disordered	6
Sr_2ZrMnO_6	ferroelectric loop at RT	53.2	$Pnma$ (RT)		7
Y_2FeCrO_6	above 260	260	$Pnma$ (350 K, 2 K)	disordered	8
Dy_2FeCrO_6	500	250	$Pnma$ (RT)	disordered	9
$CaMnTi_2O_6$	630	10	$P4_2mc$	ordered	10
		type II multiferroics			
Lu_2MnCoO_6	35	43	$P2_1/n$ (4 K, 100 K)	ordered	11
Y_2NiMnO_6	67	67	$P2_1/n$ (RT)	ordered	12
Y_2CoMnO_6	80	80	$P2_1/n$ (RT)	ordered	13

Cr_2O_3 was calcined at 1423 K for 4 h. Phase purity of the sample was confirmed by powder X-ray diffraction using Bruker D8-advanced X-ray (Cu Kα) diffractometer. Magnetization measurements were performed using a physical property measurement system (PPMS; model Evercool II from Quantum Design Inc.) in a magnetic field of 0.1 T. Field-cooled (FC) and zero-field-cooled (ZFC) magnetization data were collected in the temperature interval of 10−400 K. Magnetic hysteresis loops were measured at 50, 150, and 300 K in a magnetic field H, where $-5\ T \leq H \leq +5$ T. Dielectric constant of the sintered pellets was measured in the frequency range from 100 Hz to 1 MHz at temperatures between 573 and 300 K using the Agilent E4980A LCR meter. Ferroelectric hysteresis loop of Pr_2FeCrO_6 was measured at room temperature (RT) using precision P−E hysteresis loop tracer system (MarineIndia). X-ray photoemission spectroscopy (XPS) experiments were performed on Pr_2FeCrO_6 compound using Omicron Multiprobe Surface Science System, equipped with monochromatic source (XM 1000) and a hemispherical electron energy analyzer (EA 125). Throughout the experiment, photoemission spectra were studied at an average base pressure of $\sim 2.8 \times 10^{-11}$ Torr with power of 300 W. The total energy resolution, estimated from the width of the Fermi edge, was ~0.25 eV for monochromatic Al Kα line with photon energy of 1486.70 eV. The pass energy for core-level spectra was kept at 30 eV. Ar ion sputtering was performed at 2 keV by maintaining extractor pressure of 25 mPa. ^{57}Fe Mössbauer measurements were performed in transmission mode with ^{57}Co radioactive source in constant acceleration mode using standard personal computer (PC)-based Mössbauer spectrometer equipped with Wissel velocity drive. Velocity calibration of the spectrometer was done with the natural iron absorber at room temperature. Low-temperature ^{57}Fe Mössbauer measurements were performed using a Janis CCR. The spectra were analyzed with NORMOS program.

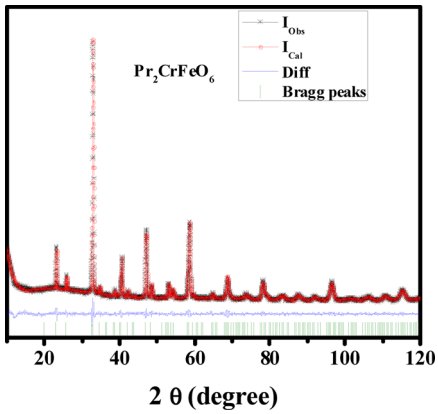

Figure 1. Rietveld refinement profile of Pr_2FeCrO_6 obtained from PXRD data. (×) Observed, (○) calculated, and (blue) difference, respectively. Bragg positions are denoted by green bars.

Table 2. Refined Lattice Parameters, Average Bond Length, and Bond Angle of Pr_2FeCrO_6

a (Å)	5.4758(4)
b (Å)	5.5094(3)
c (Å)	7.7314(4)
Fe/Cr−O (Å)	1.753(2)
Pr−O (Å)	2.334(3)
Fe/Cr−O1−Fe/Cr (deg)	157.348(1)
Fe/Cr−O2−Fe/Cr (deg)	162.187(2)

RESULTS AND DISCUSSION

Crystallography/Structural Aspects. Powder X-ray diffraction pattern suggests perovskite-type orthorhombic structure with unit cell parameters $a/b/c \approx \sqrt{2}\ a_p/\sqrt{2}\ a_p/2\ a_p$ (a_p = 3.9 Å, parameter of the perovskite subcell). Systematic absence of the diffraction lines $0kl$, $k + l \neq 2n$ and $hk0$, $h \neq 2n$ suggest space group $Pbnm$ (No. 62). Figure 1 shows refined powder X-ray diffraction (PXRD) pattern of Pr_2FeCrO_6. The refined lattice parameters, bond lengths, and bond angles are given in Table 2. All the crystallographic data, occupancies, reliability factors, and the goodness of fit (GOF) are given in Table 3. The refinement of our data allows us to conclude that Fe and Cr are randomly distributed in the two B sites (B and B′). This conclusion receives support from the fact that both Fe and Cr are in the same valence state, namely, +3, as we determined from our XPS data described below. Andersen et al.[14] have discussed the structural implications of the two B-site ions having the same valence state. One important effect is that, due to random distribution of the two B-ions, the structure becomes centrosymmetric. Our refinement analysis shows that Pr_2FeCrO_6 belongs to orthorhombic $GdFeO_3$-type centrosymmetric structure with Glazer notation $a^+a^-b^-$ tilt system.[15,16] A three-dimensional crystal structure of Pr_2FeCrO_6 is shown in Figure 2.

The small size of the A-site cation is responsible for the deviation of the structure of Pr_2FeCrO_6 from cubic to orthorhombic structure. We calculate the octahedral distortion using the formula $\Phi = (180 - \theta)/2$, where θ is the average Fe/Cr−O−Fe/Cr bond angle.[17] The value of $\Phi = 11.2°$ indicates that the octahedra are slightly distorted from the equilibrium position.

Valence States of Pr, Fe, Cr, and O from XPS Spectra. X-ray photoemission experiments performed at room temperature on our compound are shown in Figure 3a−e. Figure 3a

DOI: 10.1021/acs.inorgchem.7b01086
Inorg. Chem. 2017, 56, 12712−12718

Table 3. Structural Parameters, Reliability Parameter Obtained from Rietveld Refinement of Pr_2FeCrO_6 Using PXRD Data[a]

site	x	y	z	atom	occ	Beq (Å^2)
4c	0.008(1)	−0.0371(4)	0.25	Pr	1	0.32(4)
4b	0.5	0	0	Fe/Cr	0.5/0.5	0.15(2)
4c	−0.082(1)	0.512(1)	0.25	O1	1	0.55(7)
8d	0.195(4)	0.244(5)	0.062(4)	O2	1	0.55(7)

[a]Space group = *Pbnm* (No. 62), R_p(%) = 3.75, R_{wp} (%) = 4.29, GOF = 1.62, Z = 2, V (Å)^3 = 233.25 (4).

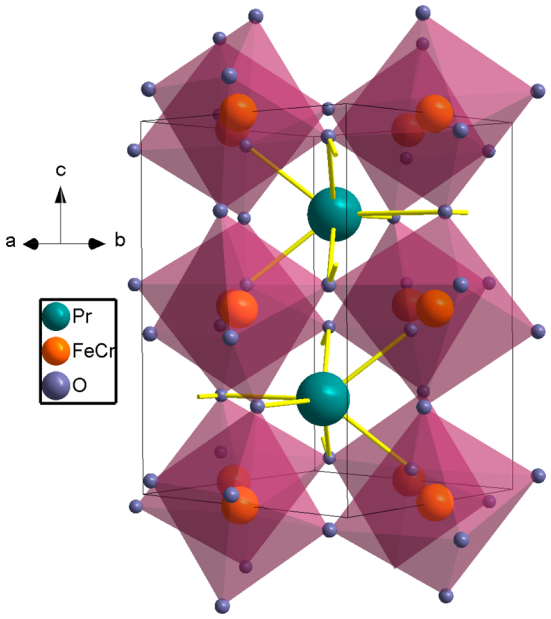

Figure 2. A perspective view of the crystal structure of Pr_2FeCrO_6. Large spheres represent Pr atoms; Fe and Cr atoms are at the center of the octahedra.

shows survey scan spectra of Pr_2FeCrO_6. Binding energy values are in good agreement with the National Institute of Standards and Technology (NIST) database, which was used to assign the position of the peaks and the spin−orbit doublet separations.[18] Pr 3d core-level spectra shown in Figure 3a comprise two well-separated spin−orbit split peaks Pr($3d_{3/2}$) and Pr($3d_{5/2}$) at 953.37 and 932.87 eV, respectively. At low-energy side of the $Pr3d_{3/2}$ and $Pr3d_{5/2}$ main lines, there are weak lines known as shakedown satellites and correspond to the Pr $3d^94f^3$ final states.[19−21] The core-level XPS Cr2p spectra reveal spin−orbit split $2p_{3/2}$ and $2p_{1/2}$ lines (Figure 3c). The Cr $2p_{3/2}$ and $2p_{1/2}$ appear at 575.8 and 585.51 eV. This doublet separation of 9.71 eV suggests that Cr exists in +3 oxidation state. Figure 3d shows the core-level spectra of Fe 2p region. Spin−orbit split $2p_{3/2}$ and $2p_{1/2}$ appear at 710.23 and 724.05 eV, respectively, with doublet separation of 13.82 eV. This corresponds to the +3 oxidation state of Fe. The satellite peak appearing at 718.6 eV in the Fe XPS data is the diagnostic signature of Fe^{3+}. In the core-level O1s spectra (Figure 3e), the peak at 528.85 eV is the characteristic peak of O^{2-} ions of the lattice oxygen, while the broad peak around 531.35 eV denotes O1s lateral structure. This lateral broad peak corresponds to the ionization of weakly adsorbed species[22] and also the ionizations of oxygen ions with particular coordinates, more specifically integrated in the subsurface. This suggests the subsurface consists of oxygen ions that bear lower electron density than the "O^{2-}" ions. Normally, these oxide ions can be described as "O^-" species or excess oxygen.[23]

We calculated bond valence sum (BVS) of Fe and Cr atoms using Fe−O and Cr−O bond lengths obtained from the refined X-ray data (Table 2). The valence can be calculated as the sum of the individual bond valences, $s_i = \exp\{(r_0 - r_i)/B\}$, where B is an empirical constant, typically = 0.37 Å,[24] and r_i and r_0 are calculated and theoretical M−O bond length. r_0 for Fe−O and Cr−O are 1.759 and 1.724 Å,[25] respectively. BVS calculations show the valence of Fe and Cr is close to 3, consistent with that determined from the XPS measurements.

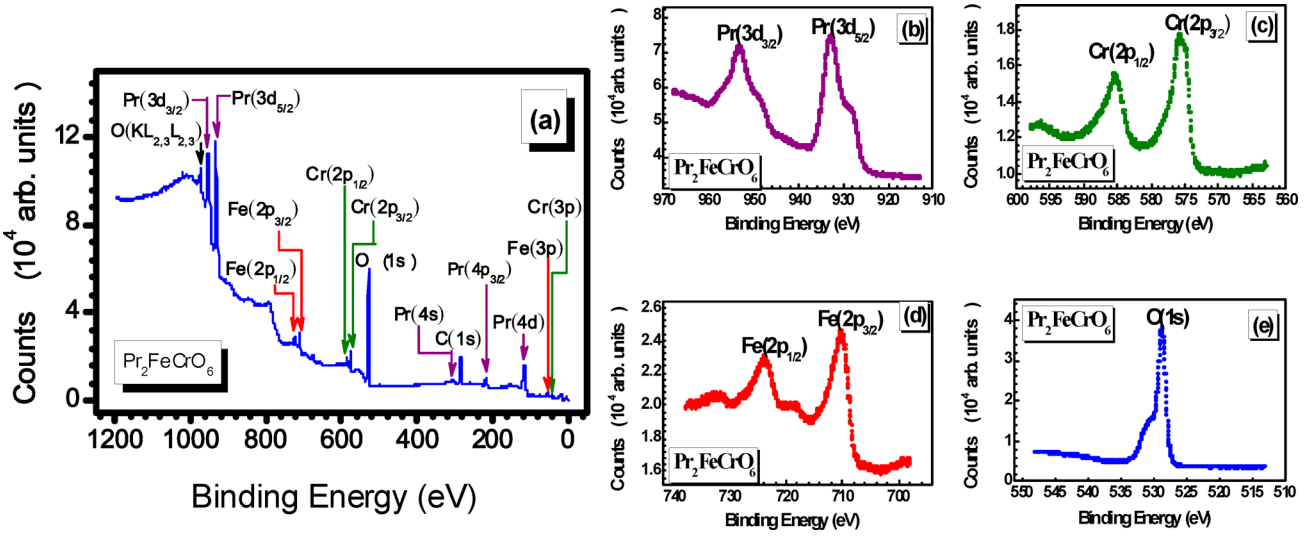

Figure 3. (a) Survey scan, (b) Pr 3d, (c) Cr 2p, (d) Fe 2p, and (e) O1s core-level X-ray photoemission spectra of Pr_2FeCrO_6 studied at room temperature.

DOI: 10.1021/acs.inorgchem.7b01086
Inorg. Chem. 2017, 56, 12712−12718

Magnetic Properties. Magnetic measurements of Pr_2FeCrO_6 were performed using vibrating sample magnetometer (VSM). Figure 4 shows the FC and ZFC magnetic

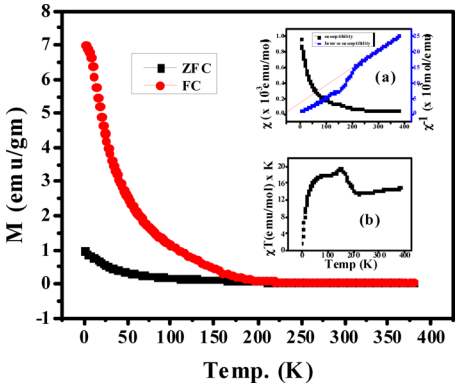

Figure 4. ZFC and FC magnetization of Pr_2FeCrO_6 as a function of temperature measured in a magnetic field of 0.1 T. (inset (a)) The magnetic susceptibility and inverse susceptibility of Pr_2FeCrO_6. (inset (b)) χT vs T plot of Pr_2FeCrO_6.

susceptibility, $\chi(T)$, from 2 to 400 K in an applied magnetic field of 0.1 T. A rapid increase in the measured magnetization M is observed below 190 K. The inverse susceptibility plot (inset (a) of Figure 4) suggests a transition from paramagnetic to a magnetically ordered state below ~240 K, which is also reflected in χT versus T plot shown in the inset (b) of Figure 4.

According to the Goodenough–Kanamori rules[26] with high-spin Fe^{3+} (t_{2g}^3 e_g^2) and Cr^{3+} (t_{2g}^3 e_g^0) the 180° superexchange interaction between one half-filled d orbital and other empty d orbital through an anion results in ferromagnetic interaction. These rules state that due to greater cation–anion interaction, the interaction between e_g orbitals will dominate over the interaction between t_{2g} orbitals. As pointed out above, Fe^{3+} and Cr^{3+} are disordered at B sites (B and B′). A long-range order among Fe^{3+} and Cr^{3+} sites, as implied by the sequence $Fe^{+3}O-Cr^{+3}O-Fe^{+3}O-Cr^{+3}O-Fe^{3+}$ is not possible. In the absence of long-range order, species such as $Fe^{+3}O-Fe^{3+}$ (e_g^2-O-e_g^2), $Fe^{+3}O-Cr^{3+}$ (e_g^2-O-e_g^0), $Cr^{+3}O-Cr^{3+}$ (e_g^0-O-e_g^0) would exist in the material. Despite this disorder among Fe^{3+} and Cr^{3+} ions the material exhibits a ferrimagnetic or weakly ferromagnetic transition as revealed by our observation of a magnetic hysteresis loop with rather low remnant magnetization, as shown in Figure 5. The observed ferrimagnetism could be G-type antiferromagnetism (AFM; a small canting to allow for weak ferromagnetism) below transition temperature.[27] The Curie–Weiss law [$\chi = C/(T - \theta)$] was used to fit the susceptibility in paramagnetic region from 400 to 244 K. The negative extrapolated temperature θ_W (−73 K) is suggestive of an antiferromagnetic ordering, which is consistent with the nearly compensated magnetic structure (low magnetic moment), as we pointed out above. The paramagnetic moment calculated from our susceptibility data is 8.3 μ_B per formula unit. This may be compared with the calculated value 8.6 μ_B using the individual ionic moments as μ_{Pr}^{+3} = 3.5 μ_B, μ_{Fe}^{+3} = 5.92 μ_B, and μ_{Cr}^{+3} = 3.87 μ_B.[28] Field-dependent magnetization measured at 5 T field and at three different temperatures 300, 150, and 50 K is shown in Figure 5. Magnetic hysteresis loop was observed at 150 and 50 K, which indicates the overall ferromagnetic nature of the compound.

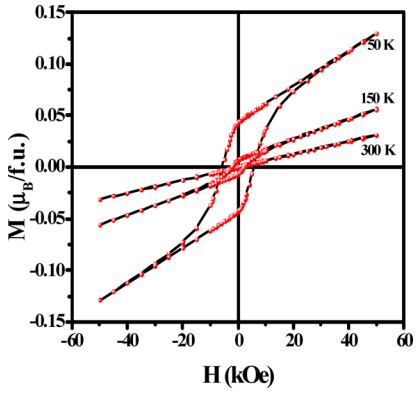

Figure 5. Isothermal magnetization of Pr_2FeCrO_6 measured at three different temperatures 300, 150, and 50 K in an applied magnetic field of 5 T.

Mössbauer Spectroscopic Studies. ^{57}Fe Mössbauer spectra of Pr_2FeCrO_6 at several temperatures are shown in Figure 6a. Our analysis of the room-temperature spectrum, which apparently is a single line, suggests that the spectrum is actually a nonresolved doublet with quadruple splitting of ~0.21 ± 0.04 mm/s and no magnetic splitting thereby indicating that the material has a noncubic structure and that the compound is paramagnetic at room temperature. The observed isomer shift of 0.37 ± 0.02 mm/s indicates the presence of Fe^{3+},[29] which is consistent with the results of our other measurements. The spectrum at 25 K is fit to a sextet, and the obtained center shift and internal hyperfine field values are 0.48 ± 0.01 mm/s and 53.0 ± 0.1 T respectively. Similar values corresponding to Fe^{3+} have been observed in other double perovskites such as Sr_2FeMoO_6.[30] From this hyperfine field we estimate the magnetic moment ~6–7 μ_B on Fe^{3+} ion in this material. This magnetic moment was calculated on the basis of an empirical relationship[31] between the hyperfine field on Fe nucleus and the magnetic moment, and by its nature this relationship is only suggested but not accurate. However, this is not too far from the moment of free Fe^{3+} in the high-spin state. Data above 150 K are fit with a distribution of hyperfine fields as shown in Figure 6. From the low-temperature Mössbauer data, internal hyperfine field is estimated and is plotted as a function of temperature as shown in Figure 6b.

The spectra below 250 K show remarkable temperature-dependent phenomena occurring in the material. There is magnetic hyperfine field at the Fe nucleus appearing at $T \leq 250$ K. In a narrow range of temperature, 260 K < T < 220 K, interesting relaxation effects associated with Fe moment dynamic fluctuations are observed.[32] Well split, but with dynamically induced line-broadening, six-finger pattern of Fe-site spectrum is observed at 200 K and down to 100 K. Hyperfine field (HF) split sharp Mössbauer spectra are observed at and below ~100 K. At 25 K, the HF at the Fe nucleus is ~53 T.

Ferroelectricity and Multiferroicity. We investigated the dielectric properties of sintered pellets from 300 to 573 K applying alternating-current (ac) field from 100 Hz to 2 MHz frequency range. The variation of dielectric constant with temperature at different frequencies is shown in Figure 7. Anomaly observed at 453 K indicates a ferroelectric to paraelectric phase transition. Ferroelectricity in our sample is clearly observed in our electric polarization measurements of Pr_2FeCrO_6 in an applied electric field. Figure 8 shows the

DOI: 10.1021/acs.inorgchem.7b01086
Inorg. Chem. 2017, 56, 12712–12718

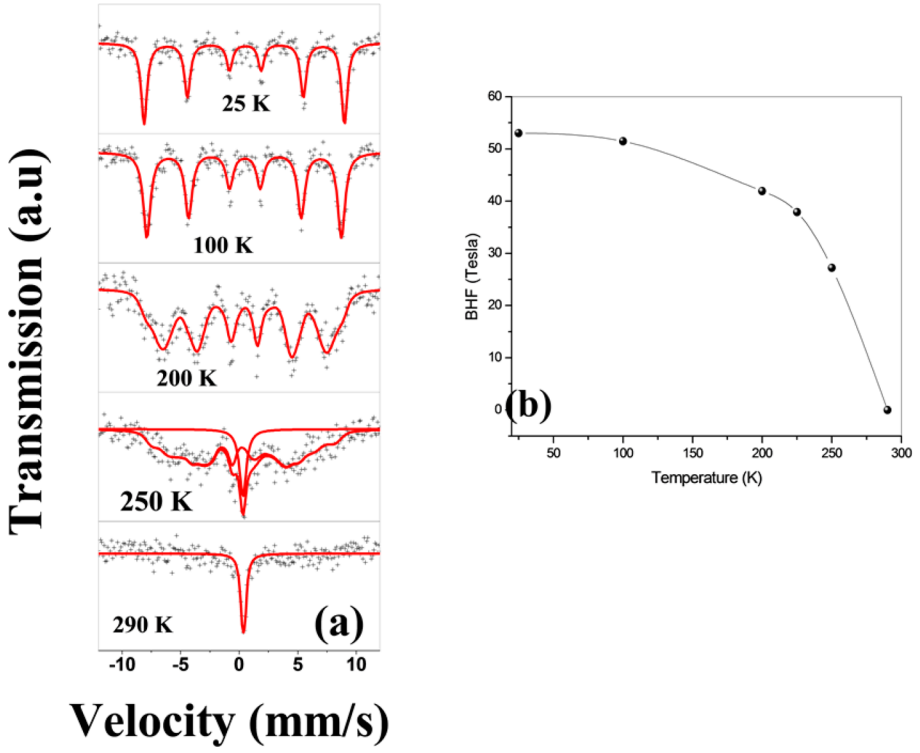

Figure 6. (a) ^{57}Fe Mössbauer spectra of Pr_2FeCrO_6 at several temperatures. The spectrum at 250 K, compared with the spectra at 290 and 200 K, suggests the presence of magnetic relaxation effects. Detailed study of these effects would be studied in our further studies. (b) Average hyperfine field as observed from fits of Mössbauer spectra.

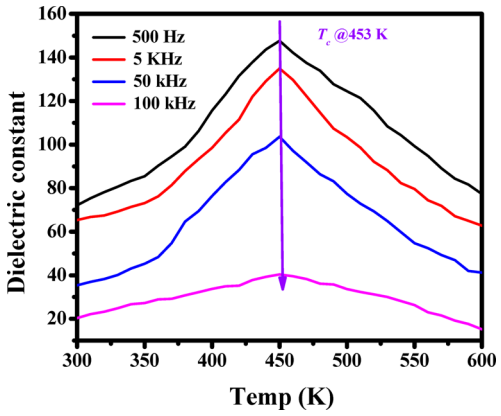

Figure 7. Temperature-dependent dielectric constant of Pr_2FeCrO_6 measured at different frequencies.

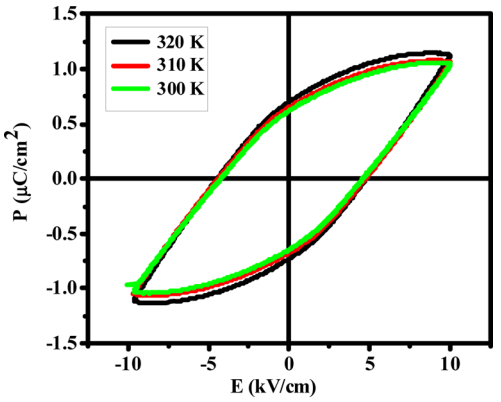

Figure 8. Ferroelectric hysteresis loop of Pr_2FeCrO_6 at three different temperatures 300, 310, and 320 K under the field of 12 kV cm^{-1}.

ferroelectric hysteresis loop of Pr_2FeCrO_6 at three temperatures 300, 310, and 320 K. The loops are nearly symmetric and well-formed. The values of the saturation polarization P_S and coercivity E_c, as obtained from the observed loops, are 1.04 μC/cm^2 with 4.77 kV/cm, respectively. The remnant polarization as we note from Figure 8 is ~0.6 μC/cm^2, which is much smaller than in $CaMnTi_2O_6$[10] (3.5 μC/cm^2). The hysteresis loop could not be observed at higher temperatures due to increase in the leakage current. To the best of our knowledge very few double perovskite materials have been reported exhibiting ferroelectric hysteresis loop. One such example is $CaMnTi_2O_6$, as we noted above. In our case, observation of hysteresis loop becomes particularly noteworthy, as P_S in our case is very small; it is several times smaller than in $CaMnTi_2O_6$. We must also point out that the structure of the compound $CaMnTi_2O_6$ from X-ray diffraction pattern was determined to be centrosymmetric, space group $P4_2/nmc$, despite its P_S being so high as compared with P_S in our material. Occurrence of ferroelectricity in most double perovskite ferroelectrics was inferred from the measurements of pyroelectric and oscillation current,[12,13] as hysteresis loop was not observed because of high leakage current.

We must point out that the space group *Pbnm* of the structure of our material Pr_2FeCrO_6, as derived from X-ray data, is centrosymmetric. Such a space group is inconsistent with the ferroelectric nature of the compound. We believe this apparent inconsistency may be resolved considering that Fe and Cr ions are randomly distributed over the two sites B and B′. The bulk of compound, due to this disorder, is rendered centrosymmetric,[33] as we see in our X-ray diffraction. Dy_2FeCrO_6[9] is another such example. In their work, the authors[9] emphasize that the material is centrosymmetric as

DOI: 10.1021/acs.inorgchem.7b01086
Inorg. Chem. 2017, 56, 12712−12718

inferred from their X-ray diffraction. However, they observe ferroelectricity at room temperature.

However, it is entirely conceivable that there are micro-regions in the material where the two sites are locally ordered giving rise to *local* non-centrosymmetric structure. Such embedded regions in the bulk of the material would be ferroelectric. As relative fraction of such regions is small, we see no diffraction lines corresponding to this ordered structure. This explains also the weak P_S in our case. In support of this conjecture, we point out that recent observation of local non-centrosymmetry has been reported in weakly biferroic $YCrO_3$.[34] We believe such a scenario exists, for example, in Y_2FeCrO_6[8] and Dy_2FeCrO_6.[9] The other possibility of explaining low P_S is that P_S arises due to ionic displacements just as it does in well-known displacive ferroelectrics. But these displacements have to be small, consistent with low value of P_S. Though the symmetry is broken due to these ionic displacements (the material becomes non-centrosymmetric), the displacements are small. We think our material is an ideal material to investigate all these subtle issues. Our work is in progress.

CONCLUSION

A disordered double perovskite material Pr_2FeCrO_6 has been synthesized as a single phase by solid-state method at 1100 °C. The PXRD refined data suggests orthorhombic *Pbnm* structure. XPS data show that all the cations have +3 oxidation state. Magnetization studies of Pr_2FeCrO_6 show that material is paramagnetic at room temperature and undergoes a magnetic transition below 250 K. We observe clear magnetic hysteresis loop, for example, below 150 K. A low remnant magnetization M_r, ∼0.05 μ_B/f. u., is inferred from the observed magnetic hysteresis loop. ^{57}Fe Mössbauer study at 25 K shows a high hyperfine magnetic field of ∼53 T at the Fe nucleus that corresponds to a magnetic moment of ∼6−7 μ_B/Fe. Interesting magnetic relaxation effects are observed close to the ferrimagnetic ordering temperature. We investigated the ferroelectric nature of the compound. The dielectric anomaly at 453 K and formation of hysteresis loop suggests that the compound is ferroelectric above room temperature. The P_S of the compound 1.04 $\mu C/cm^2$ is small in comparison to other reported ferroelectric compounds. We feel that the small value of saturation polarization is due to the local non-centrosymmetric structure of the compound. Pr_2FeCrO_6 has interesting ferroelectric and ferrimagnetic properties and is a type I multiferroic material.

AUTHOR INFORMATION

Corresponding Author

*E-mail: ashok@chemistry.iitd.ernet.in. Fax: +91-26854715.

ORCID

Satyendra Singh: 0000-0002-3648-7637

Amish G. Joshi: 0000-0002-7981-6648

Ashok Kumar Ganguli: 0000-0003-4375-6353

Present Address

[+]Visiting scientist, Dept. of Chemistry, IIT Delhi.

Notes

The authors declare no competing financial interest.

ACKNOWLEDGMENTS

The authors thank DST for the PPMS facility at the department of Physics, IIT Delhi. A.K.G. thanks DST for providing financial support.

REFERENCES

(1) Eerenstein, W.; Mathur, N. D.; Scott, J. F. Multiferroic and magnetoelectric materials. *Nature* **2006**, *442*, 759−765.

(2) Ramesh, R.; Spaldin, N. A. Multiferroics: progress and prospects in thin films. *Nat. Mater.* **2007**, *6*, 21−29.

(3) Zhang, G. Q.; Dong, S.; Yan, Z.; Guo, Y.; Zhang, Q.; Yunoki, S.; Dagotto, E.; Liu, J. M. Multiferroic properties of $CaMn_7O_{12}$. *Phys. Rev. B: Condens. Matter Mater. Phys.* **2011**, *84*, 174413−174418.

(4) Azuma, M.; Takata, K.; Saito, T.; Ishiwata, S.; Shimakawa, Y.; Takano, M. Designed Ferromagnetic, Ferroelectric Bi_2NiMnO_6. *J. Am. Chem. Soc.* **2005**, *127*, 8889−8892.

(5) Zhu, J.; Feng, S.; Liu, Q.; Zhang, J.; Xu, H.; Li, Y.; Li, X.; Liu, J.; Huang, Q.; Zhao, Y.; Jin, C. Temperature and pressure effects of multiferroic Bi_2NiTiO_6 compound. *J. Appl. Phys.* **2013**, *113*, 143514−143520.

(6) Liu, F.; Li, J.; Li, Q.; Wang, Y.; Zhao, X.; Hua, Y.; Wang, C.; Liu, X. High pressure synthesis, structure, and multiferroic properties of two perovskite compounds. Y_2FeMnO_6 and Y_2CrMnO_6. *Dalton Trans.* **2014**, *43*, 1691−1698.

(7) Landínez Téllez, D. A.; Llamosa, P. D.; Deluque Toro, C. E.; Gil Rebaza, A. V.; Roa-Rojas, J. Structural, magnetic, multiferroic and electronic properties of Sr_2ZrMnO_6 double perovskite. *J. Mol. Struct.* **2013**, *1034*, 233−237.

(8) Rajeswaran, B.; Mandal, P.; Saha, R.; Suard, E.; Sundaresan, A.; Rao, C. N. R. Ferroelectricity Induced by Cations of Nonequivalent Spins Disordered in the Weakly Ferromagnetic Perovskites, $YCr_{1-x}MxO_3$ (M = Fe or Mn). *Chem. Mater.* **2012**, *24*, 3591−3595.

(9) Nair, V. G.; Pal, L.; Subramanian, V.; Santhosh, P. N. Structural, magnetic, and magnetodielectric studies of metamagnetic $DyFe_{0.5}Cr_{0.5}O_3$. *J. Appl. Phys.* **2014**, *115*, 17D728−17D731.

(10) Aimi, A.; Mori, D.; Hiraki, H.; Takahashi, T.; Shan, Y. J.; Shirako, Y.; Zhou, J.; Inaguma, Y. High-Pressure Synthesis of A-Site Ordered Double Perovskite $CaMnTi_2O_6$ and Ferroelectricity Driven by Coupling of A-Site Ordering and the Second-Order Jahn−Teller Effect. *Chem. Mater.* **2014**, *26*, 2601−2608.

(11) Yanez-Vilar, S.; Mun, E. D.; Zapf, V. S.; Ueland, B. G.; Gardner, J. S.; Thompson, J. D.; Singleton, J.; Sánchez-Andújar, M.; Mira, J.; Biskup, N.; Señarís-Rodríguez, M. A.; Batista, C. D. Multiferroic behavior in the double-perovskite Lu_2MnCoO_6. *Phys. Rev. B: Condens. Matter Mater. Phys.* **2011**, *84*, 134427−134435.

(12) Su, J.; Yang, Z. Z.; Lu, X. M.; Zhang, J. T.; Gu, L.; Lu, C. J.; Li, Q. C.; Liu, J.-M.; Zhu, J. S. Magnetism-driven ferroelectricity in double perovskite Y_2NiMnO_6. *ACS Appl. Mater. Interfaces* **2015**, *7*, 13260−13265.

(13) Sharma, G.; Saha, J.; Kaushik, S. D.; Siruguri, V.; Patnaik, S. Magnetism driven ferroelectricity above liquid nitrogen temperature in Y_2CoMnO_6. *Appl. Phys. Lett.* **2013**, *103*, 012903−012907.

(14) Anderson, M. T.; Greenwood, K. B.; Taylor, G. A.; Poeppelmeier, K. R. B-cation arrangement in double perovskites. *Prog. Solid State Chem.* **1993**, *22*, 197−233.

(15) Glazer, A. M. Simple ways of determining perovskite structures. *Acta Crystallogr., Sect. A: Cryst. Phys., Diffr., Theor. Gen. Crystallogr.* **1975**, *31*, 756−762.

(16) Glazer, A. M. The classification of tilted octahedra in perovskites. *Acta Crystallogr., Sect. B: Struct. Crystallogr. Cryst. Chem.* **1972**, *28*, 3384−3392.

(17) Muñoz, A.; Alonso, J. A.; Casais, M. T.; Martínez-Lope, M. J.; Fernández-Díaz, M. Crystal and Magnetic Structure of the Complex Oxides Sr_2MnMoO_6, Sr_2MnWO_6 and Ca_2MnWO_6: A Neutron Diffraction Study. *J. Phys.: Condens. Matter.* **2002**, *14*, 8817−8832.

(18) See, A. V.; Naumkin, A. K.; Vass, S.; Gaarenstroom, W.; Powell, C. J. For (compilation and evaluation), NIST Standard Reference Database 20, Version 4.1: http://srdata.nist.gov/xps/.

(19) Fuggle, J. C.; Hillebrecht, F. U.; Zołnierek, Z.; Lässer, R.; Freiburg, C.; Gunnarsson, O.; Schönhammer, K. Electronic structure of Ce and its intermetallic compounds. *Phys. Rev. B: Condens. Matter Mater. Phys.* **1983**, *27*, 7330−7341.

(20) Szytuła, A.; Penc, B.; Jezierski, A. XPS study of $RNiSb_2$ (R = Pr, Nd). *Mater. Sci. Poland* **2008**, *26*, 759−765.

DOI: 10.1021/acs.inorgchem.7b01086
Inorg. Chem. 2017, 56, 12712−12718

(21) Toliński, T.; Kowalczyk, A.; Chełkowska, G. XPS studies of the hybridization effects in RNi_4B (R = Ce, Pr, Nd) compounds. *Phys. Lett. A* **2003**, *308*, 75−79.
(22) Cao, W.; Tan, O. K.; Zhu, W.; Pan, J. S.; Bin, J. Study of xα-Fe_2O_3-(1-x)ZrO_2 solid solution for low-temperature resistive oxygen gas sensors. *IEEE Sens. J.* **2003**, *3*, 421−434.
(23) Dupin, J. C.; Gonbeau, D.; Vinatier, P.; Levasseur, A. Systematic XPS studies of metal oxides, hydroxides and peroxides. *Phys. Chem. Chem. Phys.* **2000**, *2*, 1319−1324.
(24) Brown, I. D. Z. Modeling the structure of La_2NiO_4. *Kristallogr.* **1992**, *199*, 255−272.
(25) Brese, N. E.; O' Keeffe, M. Bond-Valence Parameters for Solids. *Acta Crystallogr., Sect. B: Struct. Sci.* **1991**, *47*, 192−197.
(26) (a) Goodenough, J. B. Theory of the Role of Covalence in the Perovskite-type Manganites [La, M(II)]MnO_3. *Phys. Rev.* **1955**, *100*, 564−572. (b) Kanamori, J. Superexchange interaction and symmetry properties of electron orbitals. *J. Phys. Chem. Solids* **1959**, *10*, 87−98.
(27) Zhao, H. J.; Bellaiche, L.; Chen, X. M.; Íñiguez, J. Improper electric polarization in simple perovskite oxides with two magnetic sublattices. *Nat. Commun.* **2017**, *8*, 14025.
(28) Antoshina, L. G.; Goryaga, A. N.; Kukudzhanova, E. N. Effect of Cr^{3+} ions on the magnetic moment of ferrites of the system $CuFe_{2-x}Cr_xO_4$. *Phys. Solid State* **1998**, *40*, 99−108.
(29) Pathak, V.; Bhardwaj, K. K.; Agrawal, A. Mossbauer spectral studies of some Fe(III)-Ketoanil complexes. *Asian J. Chem.* **2010**, *22*, 7563−7566.
(30) Lindén, J.; Yamamoto, T.; Karppinen, M.; Yamauchi, H.; Pietari, T. Evidence for valence fluctuation of fe in $SrFeMoO_6$-w double perovskite. *Appl. Phys. Lett.* **2000**, *76*, 2925−2927.
(31) Vincze, I.; Campbell, I. A.; Meyer, A. hyperfine field and magnetic moment in b.c.c. Fe-Co and Fe-Ni. *Solid State Commun.* **1974**, *15*, 1495−1497.
(32) Menéndez, N.; García-Hernández, M.; Sánchez, D.; Tornero, J. D.; Martínez, J. L.; Alonso, J. A. Charge transfer and disorder in double perovskites. *Chem. Mater.* **2004**, *16*, 3565−3572.
(33) Turp, S. A.; Hargreaves, J.; Baek, J.; Shiv Halasyamani, P.; Hayward, M. A. Noncentrosymmetric Cation Order in the Cubic Perovskite $Ba_4CaFe_3O_{9.5}$. *Chem. Mater.* **2010**, *22*, 5580−5587.
(34) Ramesha, K.; Llobet, A.; Proffen, Th.; Serrao, C. R.; Rao, C. N. R. *J. Phys.: Condens. Matter* **2007**, *19*, 102202−102210.

DOI: 10.1021/acs.inorgchem.7b01086
Inorg. Chem. 2017, 56, 12712−12718